Scientific Research Report

Identification and Validation of Ferritinophagy-Related Biomarkers in Periodontitis

Yi-Ming Li [a,†], Chen-Xi Li [b,c,†*], Reyila Jureti [a], Gulinuer Awuti [a]

[a] Department of Periodontology, School/Hospital of Stomatology, The First Affiliated Hospital of Xinjiang Medical University, National Clinical Medical Research Institute, Urumqi, China
[b] Department of Oral and Maxillofacial Oncology & Surgery, School/Hospital of Stomatology, The First Affiliated Hospital of Xinjiang Medical University, National Clinical Medical Research Institute, Urumqi, China
[c] Dental Medicine Institute of Xinjiang Uygur Autonomous Region, Urumqi, China

ARTICLE INFO

Article history:
Received 4 January 2025
Received in revised form
19 February 2025
Accepted 1 March 2025
Available online xxx

Key words:
Periodontitis
Ferritinophagy
Biomarkers
Immune infiltration profiles
Bioinformatics analyses

ABSTRACT

Objective: While ferritinophagy is believed to play a significant role in the development of periodontitis, the exact mechanisms remain unclear. This study aimed to investigate the biomarkers associated with ferritinophagy in periodontitis using transcriptomic data.

Methods: Two periodontitis-related datasets from Gene Expression Omnibus, GSE10334, and GSE16134, served as the training and validation cohorts, respectively. Additionally, 36 ferritinophagy-related genes (FRGs) were obtained from the GeneCards database. We compared the expression differences of FRGs between the periodontitis and control groups, identifying the different FRGs as candidates. Weighted gene coexpression network analysis (WGCNA) was applied to capture the key modules and modular genes related to periodontitis, utilizing the candidate FRG scores as trait. Then we intersected these with key module genes to identify differentially expressed FRGs. Hub genes were filtered using a protein-protein interaction network. Ultimately, biomarkers were acquired through machine learning, receiver operating characteristic curves, and expression levels. In addition, biomarker-associated immune cells and functional pathways were analysed to predict the upstream regulatory molecules.

Results: In total, 18 candidate FRGs showed significant differences between the periodontitis and control groups, and from the protein-protein interaction network, eight hub genes were identified among the 175 differentially expressed FRGs by analysing 1096 differentially expressed genes and 4479 key modular genes. Eventually, ALDH2, diazepam binding inhibitor, HMGCR, OXCT1, and ACAT2 were identified as potential biomarkers through machine learning algorithms, receiver operating characteristic curve analysis, and gene expression assessments. In addition, resting dendritic cells, mast cells, and follicular helper T cells were positively correlated with the five biomarkers (Cor > 0.3 and $P < .05$). All five biomarkers are involved in the translation initiation pathway, including transcription factors like KLF5 and microRNAs such as hsa-miR-495-3p and hsa-miR-27a-3p. Reverse transcription-quantitative polymerase chain reaction analysis showed that all biomarkers were expressed at low levels in the periodontitis group. However, the differences in expression levels for OXCT1 and ACAT2 between groups were not statistically significant.

Conclusions: A total of five ferritinophagy-related biomarkers – ALDH2, diazepam binding inhibitor, HMGCR, OXCT1, and ACAT2 – were screened to explore new treatment options for periodontitis.

* *Corresponding author*. Department of Oral and Maxillofacial Oncology & Surgery, School/Hospital of Stomatology, The First Affiliated Hospital of Xinjiang Medical University, National Clinical Medical Research Institute, Dental Medicine Institute of Xinjiang Uygur Autonomous Region, No. 137 Liyushan South Road, Urumqi 830054, China.
E-mail address: lichenxiuke@gmail.com (C. Li).
Chen-Xi Li: http://orcid.org/0000-0003-1443-4769
† Chen-Xi Li and Yi-Ming Li contributed equally to this work and considered co-first authors.
https://doi.org/10.1016/j.identj.2025.03.011

Introduction

Periodontitis is a chronic noncommunicable disease that affects a large number of people, making it the sixth most prevalent disease in humans.[1] As a chronic inflammatory disease, periodontitis primarily impacts the tissues that support the teeth, which include the gums, periodontal ligament, and alveolar bone. The development of periodontitis is influenced by a combination of factors, primarily including plaque biofilm, the immune response of the host, and various risk factors, which encompass environmental, genetic, and systemic issues, as well as smoking and psychological aspects.[2] The primary signs and symptoms of periodontitis are red and swollen gums, deep pockets around the teeth, gum recession, and exposed tooth roots. If not treated promptly, periodontitis can worsen and eventually lead to tooth mobility and loss, along with a decrease in chewing function, which severely impacts the patient's quality of life. Currently, the management of periodontitis mainly includes oral hygiene education, basic periodontal therapy, and surgical interventions.[3] However, these treatments can only slow or stop disease progression because they do not regenerate lost alveolar bone, and current periodontal therapies cannot achieve true anatomical healing.[4-7] Therefore, identifying biomarkers with potential diagnostic value in periodontitis will aid in the prevention and treatment of the condition, thereby improving the quality of life for patients.

Recent studies have shown that ferritinophagy plays a significant role in the pathological process of periodontitis. Specifically, it modulates inflammatory response intensity by regulating intracellular iron levels.[8] Studies reveal that higher iron levels in periodontal tissues can worsen inflammation, regulated by ferritinophagy, which breaks down ferritin and releases iron into the tissues.[9] In addition, patients with periodontitis frequently experience oxidative stress, and excess iron ions can increase free radical production, causing additional tissue damage. Ferritinophagy reduces oxidative stress by eliminating excess ferritin, which protects cells. Importantly, during the repair and regeneration of periodontal tissues, ferritinophagy plays a crucial role in regulating cell survival and death. When ferritinophagy malfunctions, it leads to increased cell death, which hinders the recovery of periodontal tissues.[10] The effects of ferritin degradation, whether protective or detrimental, crucially rely on the dynamic iron metabolism balance within cells. Specifically, in iron homeostasis or low-iron situations, ferritinophagy reduces oxidative stress and protects cells by removing excess ferritin. Conversely, in iron-overloaded circumstances, the same process might instead cause harmful effects.[11] Therefore, the function of ferritin degradation needs a comprehensive assessment based on the specific context, such as the environment, cell type, and iron's dynamic state. In summary, regulating the ferritinophagy pathway is a promising therapeutic target for periodontitis. Exploring the molecular mechanisms connecting ferritinophagy and periodontitis may clarify disease progression, and ongoing studies are investigating methods to modulate ferritinophagy through drugs or genetic interventions to alleviate periodontal inflammation and tissue destruction.[12] However, more research is needed to understand the role and molecular mechanisms of ferritinophagy in periodontitis. Thus this study aims to investigate how ferritinophagy-related genes (FRGs) may function in periodontitis.

This study utilized public transcriptomic data related to periodontitis to identify biomarkers associated with FRGs. Moreover, the study aimed to explore how these biomarkers influence the occurrence and progression of periodontitis. The goal is to develop new prevention strategies and therapeutic approaches that effectively control the disease and enhance patients' quality of life.

Materials and methods

Data source

The GSE10334 dataset (platform: GPL570) is available for download from the Gene Expression Omnibus (GEO) database (https://www.ncbi.nlm.nih.gov/geo/). It includes a total of 247 gingival tissue samples: 183 from patients with periodontitis (the periodontitis group, n = 183) and 64 from those without periodontitis (the control group, n = 64). The GSE16134 dataset (platform: GPL570) served as the validation set, consisting of 310 gingival tissue samples downloaded from the GEO database. This included 241 samples from patients with periodontitis and 69 control samples. Furthermore, we collected 36 FRGs from the GeneCards database (https://www.genecards.org/) to support our analysis. For data preprocessing, we next used the avereps function to aggregate the values of gene expression, which effectively prevents missing genes from influencing the final results.

Differential expression analysis

To characterize the expression of FRGs in periodontitis, a Wilcoxon test was conducted on FRGs based on training set, and the expression of FRGs in periodontitis and control samples was analysed using R language limma package (version 3.62.2).[13] This analysis revealed significant differences between the affected (periodontitis) and unaffected (control) sites, leading to the identification of candidate FRGs with an adjusted P value of less than .05. To estimate the differential expression of candidate FRGs between two groups, we applied the single sample gene set enrichment analysis (GSEA) algorithm using the GSVA package (version 1.48.2).[14] This approach assessed candidate FRG scores across all samples based on those obtained from the training set. We then performed group comparisons using the Wilcoxon test.

Acquisition of key modular genes

The full gene expression matrix from all samples in the training set was utilized with the WGCNA package (version 1.7-3) to construct a weighted gene coexpression network aimed at identifying key modular genes associated with periodontitis,[15] using candidate FRGs scores as a trait. Initially, outlier samples were removed through clustering to clarify the overall correlation among all samples in the training dataset, which enhances the accuracy of the analysis that follows. To guarantee that intergene interactions optimally fit the scale-free distribution, we calculate the soft threshold for the data, achieving R^2 = 0.85 and a mean connectivity that approaches

zero. Genes were then organized into distinct gene modules through hierarchical clustering. We assessed the correlations between the modules and the candidate FRGs scores using the Spearman correlation method. The two modules with the highest positive correlation and the highest negative correlation with the candidate FRGs scores were identified as key modules. The genes from these two identified modules were then combined to define the key modular genes.

Functional enrichment analysis

We performed a differential expression analysis using the limma package on the training set to identify differentially expressed genes (DEGs) between periodontitis and control samples, applying the criteria of $P < .05$ and $|\log_2$fold-change (FC)$| > 0.5$. To further investigate DEGs associated with ferritinophagy in periodontitis, we identified the intersection of DEGs and key modular genes to yield differentially expressed FRGs (DE-FRGs). Next, we functionally enriched the DE-FRGs using gene ontology (GO) and Kyoto Encyclopedia of Genes and Genomes (KEGG) analyses. We set the significance thresholds at $P < .05$ and false discovery rate < 0.05, utilizing the clusterProfiler package (version 4.4.4).[16] To explore interactions of proteins encoded by DE-FRGs, we used the STRING database (http://www/string-db.org/) to create a protein-protein interaction network for 'Homo sapiens' with an interaction score of ≥0.4. The DE-FRGs were screened using four algorithms in Cytohubba: Degree, Edge Percolated Component, Maximal Clique Centrality, and Maximum Neighborhood Component. The top 20 genes identified by these algorithms were compared, and the common genes were designated as hub genes for subsequent analyses aimed at understanding their roles.

Identification of biomarkers

To identify key genes, we applied three methods: least absolute shrinkage and selection operator (LASSO) from the glmnet package (version 4.1.4), support vector machine-recursive feature elimination (SVM-RFE) from the caret package (version 6.0-94, https://cran.r-project.org/web/packages/caret/index.html), and the Boruta algorithm from the Boruta package (version 4.3.0) to hub genes in the training set.[17,18] To evaluate the ability of key genes to distinguish between periodontitis and control samples, we plotted receiver operating characteristic (ROC) curves. This was done for both training and validation cohorts using the pROC package (version 1.18.0).[19] The area under the curve (AUC) was calculated, where values above 0.7 signify strong differentiation capability. Key genes with an AUC greater than 0.8 in both the training and validation sets were selected as candidate biomarkers for further analysis. To examine the expression of candidate biomarkers in periodontitis and control samples from both training and validation sets, we screened genes with significant expression differences ($P <$ .05) and consistent expression trends across both datasets using the Wilcoxon test.

Construction of nomogram

A nomogram model was established using the RMS package (version 6.5.0, https://CRAN.R-project.org/package=rms) to evaluate the diagnostic value of biomarkers in clinical settings. Each biomarker was scored individually, allowing to infer the incidence of periodontitis from the total score. In addition, calibration curves were plotted using regplot package to demonstrate the agreement between predicted probability of nomogram model and the actual incidence rate. Decision curve analysis (DCA) was performed using the ggDCA package (version 1.2) to evaluate the clinical benefit of the model at varying risk thresholds.[20] The accuracy of the nomogram predictions was evaluated through ROC curves (AUC > 0.7).

Immune infiltration analysis

To explore the differences in immune cell infiltration between periodontitis and control samples, we assessed the composition and abundance of 22 immune infiltrating cells in all training set samples using CIBERSORT.[21] The differences in immune cell infiltration between two groups of samples were also compared by the Wilcoxon signed-rank test. Spearman correlation analysis was performed to assess biomarkers and different immune cells across all samples in the training set, focusing on |correlation (Cor)| > 0.3 and $P < .05$.

Gene set enrichment analysis

To investigate the biological functions and pathways of biomarkers, Spearman correlation analysis was performed between each biomarker and all genes in the training set, which consisted of periodontitis and control samples, using the psych package (version 2.2.9).[22] The correlation coefficients were used to rank the biomarkers. The ClusterProfiler package was used to perform GSEA for each biomarker. For the enriched pathways, we used screening criteria of $P < .05$ and false discovery rate < 0.25, along with the reference gene set (c2.cp.kegg.v7.2.symbols.gmt).

Ferritinophagic biomarker-associated analyses

We integrated the identified biomarker-target interactions with the top 10 pathways derived from GSEA to construct the biomarker-target-pathway network using Cytoscape. Spearman analysis of biomarkers was performed based on all the samples in the training set using the psych package. The threshold was set at $|Cor| > 0.3$ and $P < .05$. Meanwhile, the GOSemSim package (version 2.28.0) was applied to assess the functional similarities among biomarkers.[23] We explored additional genes related to biomarker functions using the GeneMANIA database (http://genemania.org/), predicting associated genes and displaying the results in a gene-gene interaction network. The top 20 genes were selected as key nodes, and the five most significant pathways associated with them were highlighted. The transcription factors (TFs) for each biomarker were predicted using the ChEA3 database (https://maayanlab.cloud/chea3/), and finally, the TF-biomarker regulatory network was illustrated. The miRanda (http://www.microrna.org) and TargetScan (https://www.targetscan.org/vert_80/) databases were utilized to predict target microRNAs (miRNAs) interacting with biomarkers and constructed the complete miRNA-biomarker regulatory network with Cytoscape software. To identify drugs that target

Table – List of primer sequences for RT-qPCR.

Primer name	Sequence (5′-3′)
ALDH2	F: GGTAGCTGAAGGGGACAAGG
	R: CCTGTGTGATGCGTCCATGC
DBI	F: TGTTTCCAGCATACTGTGCC
	R: CTCATCCGATGGCTTGGTCT
HMGCR	F: TGATTGACCTTTCCAGAGCAAG
	R: CTAAAATTGCCATTCCACGAGC
OXCT1	F: TACAAGGTAAAGTGCGGGGG
	R: TTATCGCGTCTCGCTCCATC
ACAT2	F: GTGCCGCATGGTTTTCAACG
	R: GCCGCTGTAGCCCTTCTATT
GAPDH	F: CGAAGGTGGAGTCAACGGATTT
	R: ATGGGTGGAATCATATTGGAAC

RT-qPCR, reverse transcription-quantitative polymerase chain reaction.

biomarkers, we queried the Drug Gene Interaction Database (DGIdb, http://www.dgidb.org).

Reverse transcription-quantitative polymerase chain reaction (RT-qPCR) for validation

To determine the validity of biomarker expression, RT-qPCR was performed. Ten tissue samples from patients diagnosed with periodontitis and 10 samples from control individuals were used.[24,25] Periodontitis tissue samples were obtained from 10 patients with severe periodontitis diagnosed as Stage III Grade C or Stage IV Grade C according to the 2018 new classification,[26] and gingival tissues were collected from around hopeless teeth. For the control group, gingival tissues were obtained from 10 periodontally healthy individuals undergoing orthodontic extraction of premolars. The extracted teeth showed no bleeding on probing, had a probing depth of 1 to 3 mm, and no attachment loss, and tissues were collected from around these teeth. Exclusion criteria encompassed the existence of any systemic diseases.

Amplification conditions for RT-qPCR were as follows: 40 cycles, 1 minute at 95°C, 20 seconds at 95°C, 20 seconds at 55°C, and 30 seconds at 72°C. The qPCR primers were listed in Table, with GAPDH serving as the reference gene. The relative expression levels of the biomarkers were calculated using the $2^{-\Delta\Delta CT}$ method.

Statistical analyses

R software version 4.2.2 (R Foundation for Statistical Computing) was exhibited for data visualization. Differences intergroups were analysed by Wilcoxon test, with $P < .05$ as statistical significance.

Results

Significant differences in FRGs

The 36 FRGs were matched to 30 FRGs in the training set for expression level analysis, revealing that 18 candidate FRGs exhibited significantly different expression levels between the periodontitis group (affected site) and the control group (unaffected site), with 10 up-regulated and 8 down-regulated (Figure 1A). Furthermore, the analysis revealed a significant difference in candidate FRG scores, with the periodontitis group (affected site) exhibiting higher scores compared to the control group (unaffected site) (Figure 1B).

Key modular genes from key modules with periodontitis

Outlier samples (GSM261256, GSM261278, and GSM261279) were initially removed based on their clustering (Figure 2A). Subsequently, when R^2 first reached the threshold of 0.85 and the soft threshold was set to 12, the network approached a scale-free distribution, and the mean connectivity decreased towards 0 (Figure 2B). The dynamic tree-cut method identified and merged gene modules, resulting in a total of 10 modules (Figure 2C). Correlation analysis revealed that the blue module exhibited the highest negative correlation with candidate FRG scores (Cor = −0.42, $P < .0001$), while the light yellow module showed the highest positive

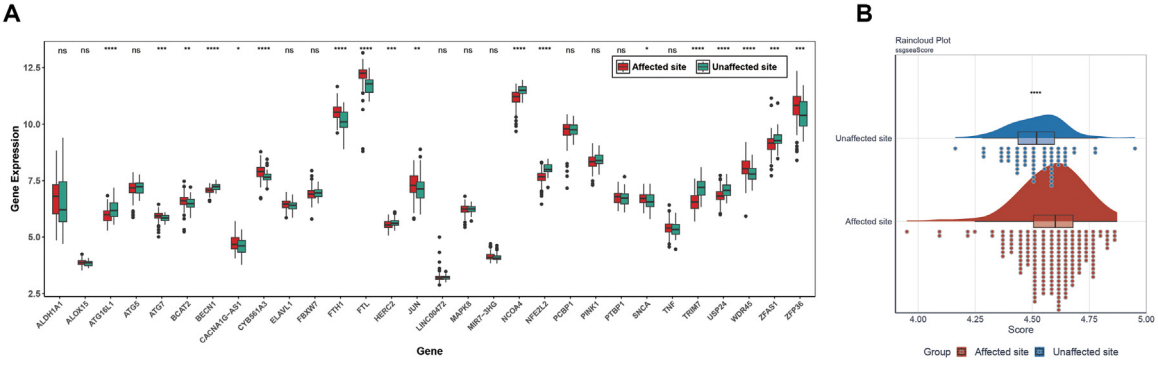

Fig. 1 – The expression level of FRGs. (A) Differential expression analysis of FRGs. The centre line of the box represented the median. The points outside the box represented outliers, and the whisks above and below the box extended to the maximum and minimum values within the nonoutlier range. 'ns': Not significant; '*': $P < .05$; '': $P < .01$; '***': $P < .001$; '****': $P < .0001$. (B) Difference FRGs score cloud-rainy map. The vertical axis represented the relative enrichment degree of FRGs in each sample. The horizontal axis represented the ssGSEA score of a single sample, with each point representing a sample, '****': $P < .0001$.**

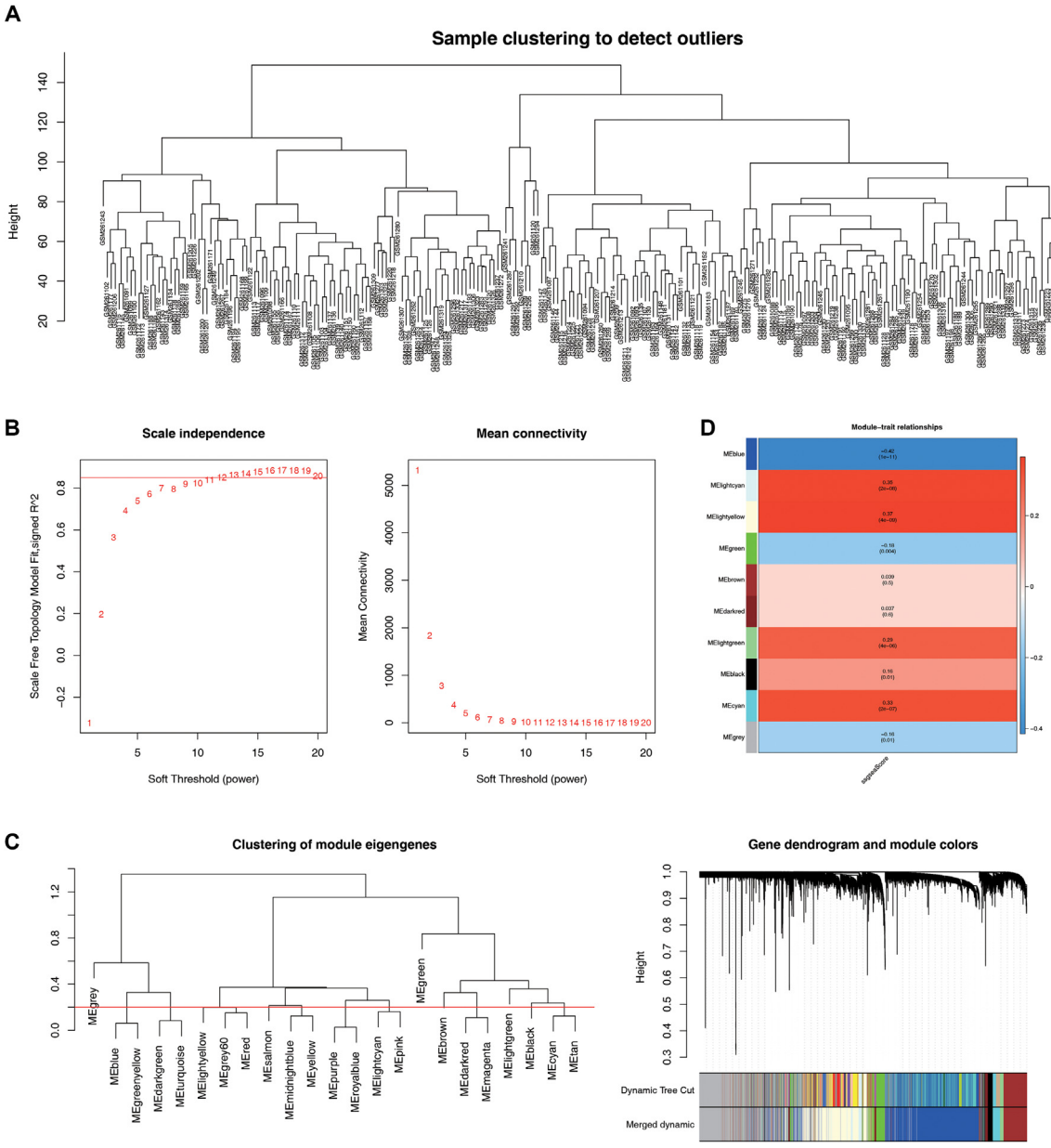

Fig. 2 – Screening of module genes by WGCNA. (A) Plot of sample clustering. (B) Determination of soft-threshold. The horizontal axis represented the weight parameter. In the left figure, the vertical axis was Scale Free Topology Model Fit, namely signed R^2, the square of the correlation coefficient R^2 between log(k) and log(p(k)) in the corresponding network. The higher the square of the correlation coefficient, the closer the network was to the scale-free network distribution. In the right figure, the vertical axis represented the average connectivity of all genes in the corresponding gene module. (C) Module genes. The clustering diagram of module-eigengenes was in the left figure. Each point represented the eigengene of a module, with its name marked; the branches of the dendrogram showed the relative distances between module-eigengenes. The gene dendrogram and module colours were in the right figure. The y-axis represented the height during gene clustering, showing the differences between genes. The coloured bars below the dendrogram showed the gene modules identified by the dynamic tree-cutting method and the subsequent module – merging results. (D) Correlation heatmap. Each row corresponded to a gene module. Blue represented negative correlation, red represented positive correlation. The deeper the colour was, the stronger the correlation was. Grey represented no correlation.

correlation (Cor = 0.37, $P < .0001$). A total of 4479 key modular genes were identified, consisting of 3108 genes from the blue module and 1371 genes from the light yellow module (Figure 2D).

Hub genes acquisition depending on DE-FRGs

A total of 1096 DEGs were identified, including 523 that were down-regulated and 573 that were up-regulated (Figure 3A,B).

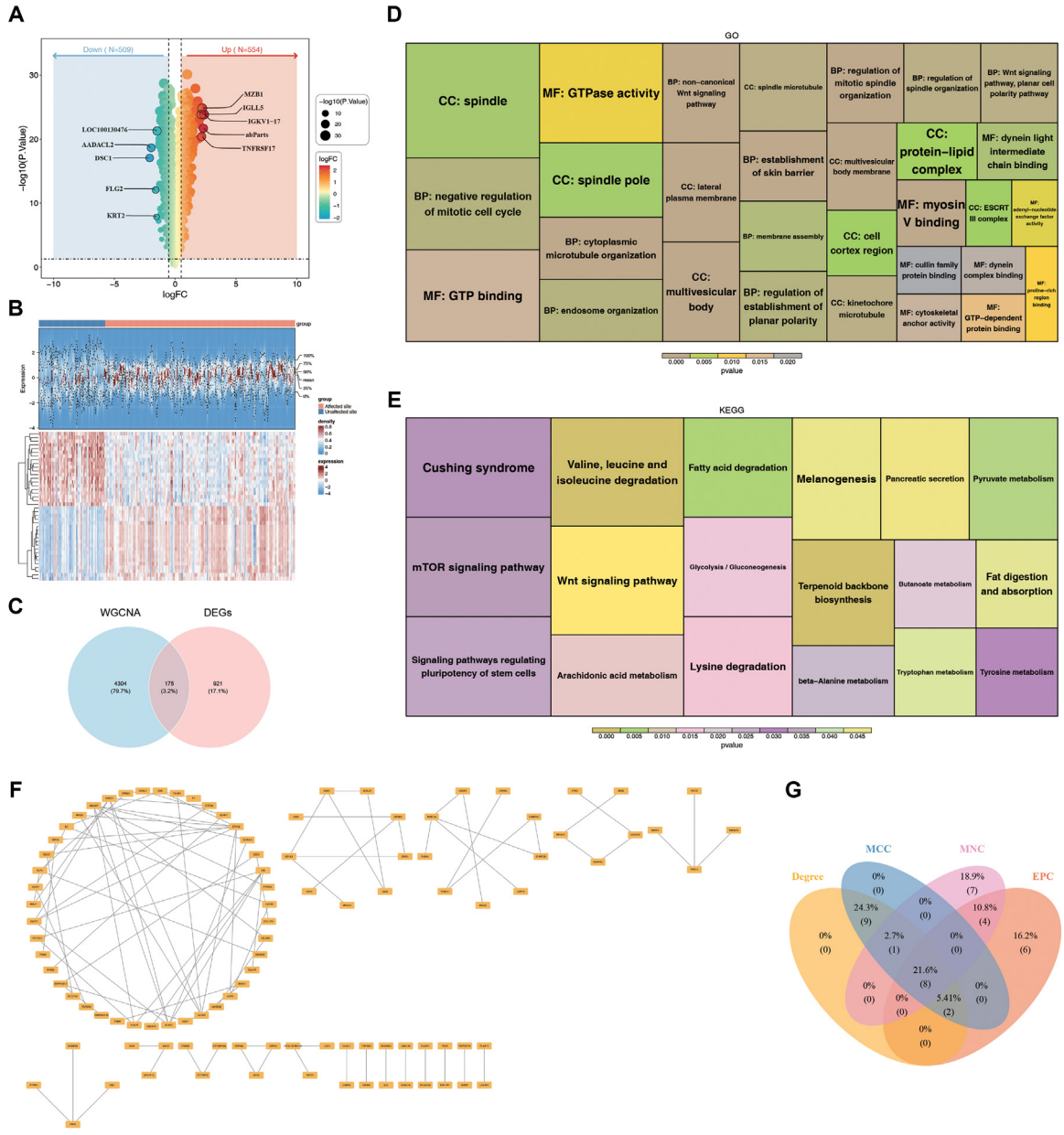

Fig. 3 – Screening and functional analysis of hub genes. (A) Volcano plot of differentially expressed genes. Blue dots represented genes with down-regulated expression, red dots represented genes with up-regulated expression, and yellow dots represented genes with no significant difference. Dots at a higher position on the vertical axis indicated expression changes with stronger statistical significance. (B) Heatmap of differentially expressed genes. Diseased tissue samples were marked in red, and control tissue samples were marked in blue. Row and column clustering of the dendrogram revealed the similarity patterns between genes and samples. The expression level changed from blue (the lowest expression level) to red (the highest expression level). (C) Venn diagram of DEGs and key module genes. (D) GO functional enrichment analysis tree diagram. Each rectangle represented a biological pathway or process. The size of the rectangle compared the relative number of each category, and the colour was arranged according to the *P* value to show statistical significance. (E) KEGG functional enrichment analysis tree diagram. (F) PPI network. (G) Venn diagram for screening hub genes by ranking the top 20 with four algorithms.

Using these DEGs, we further identified 175 DE-FRGs by interpolating them with 4479 key modular genes (Figure 3C). For DE-FRGs, GO analysis enriched 289 items, including 231 biological processes (BP), 32 cellular components, and 26 molecular functions in terms such as 'multivesicular body', 'cytoplasmic microtubule organization', and 'establishment of skin barrier' (Figure 3D). KEGG was enriched in 17 pathways, such as 'arachidonic acid metabolism', 'tryptophan metabolism', and 'melanogenesis' (Figure 3E). Moreover, the protein-protein interaction network revealed protein interactions among the DE-FRGs, comprising 120 nodes and 95 edges (Figure 3F). The top 20 genes identified by four Cytohubba

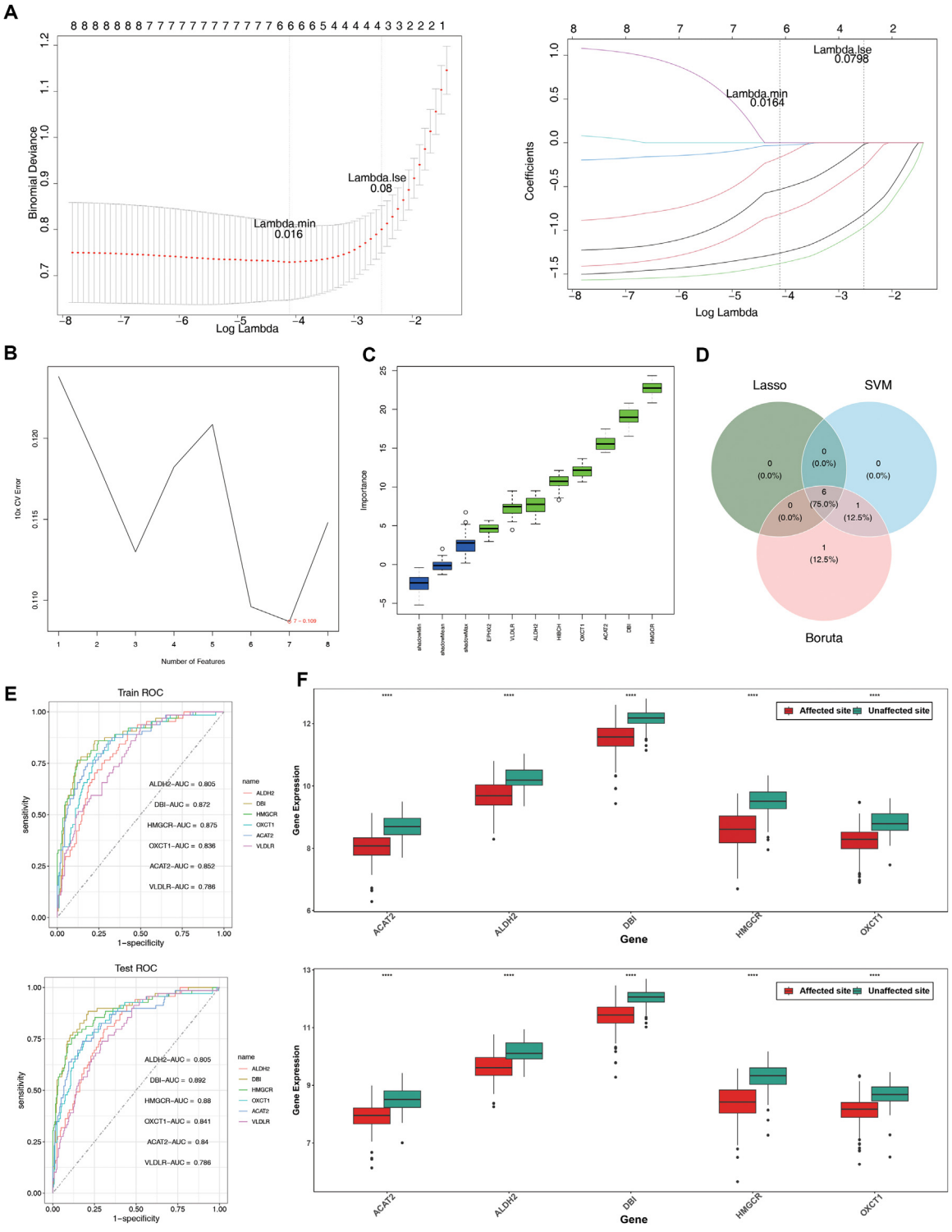

Fig. 4 – Screening and identification of biomarkers. (A) Screening of key genes by LASSO algorithm. The cross-validation error plot of the LASSO model was on the left. The selection of the λ value was based on the minimization of the cross-validation error. The first dashed line indicated 'Lambda.min'; the second dashed line marked the position of one-standard-deviation from the lowest point 'Lambda.1se', which represented the simplest model that could be obtained at the cost of one-standard-deviation. The coefficient path plot of the LASSO model was on the right. The lines tended to zero, indicating that the coefficients were compressed. (B) Screening of key genes by SVM-RFE algorithm. The y-axis represented the cross-validation (CV) error, and the x-axis represented the number of selected features. (C) Box plot of screening key genes by Boruta algorithm. Each box represented the distribution of importance score of different genes. The horizontal line within the box represented the median, and the points outside the box represented outliers. (D) Venn diagram of key genes screened by LASSO, SVM-RFE, and Boruta algorithms. (E) ROC curve plots of the training set and the test set. Each curve represented a key gene. (F) Box-plot analysis of biomarker expression levels in the training set and the validation set. '**': $P < .0001$.**

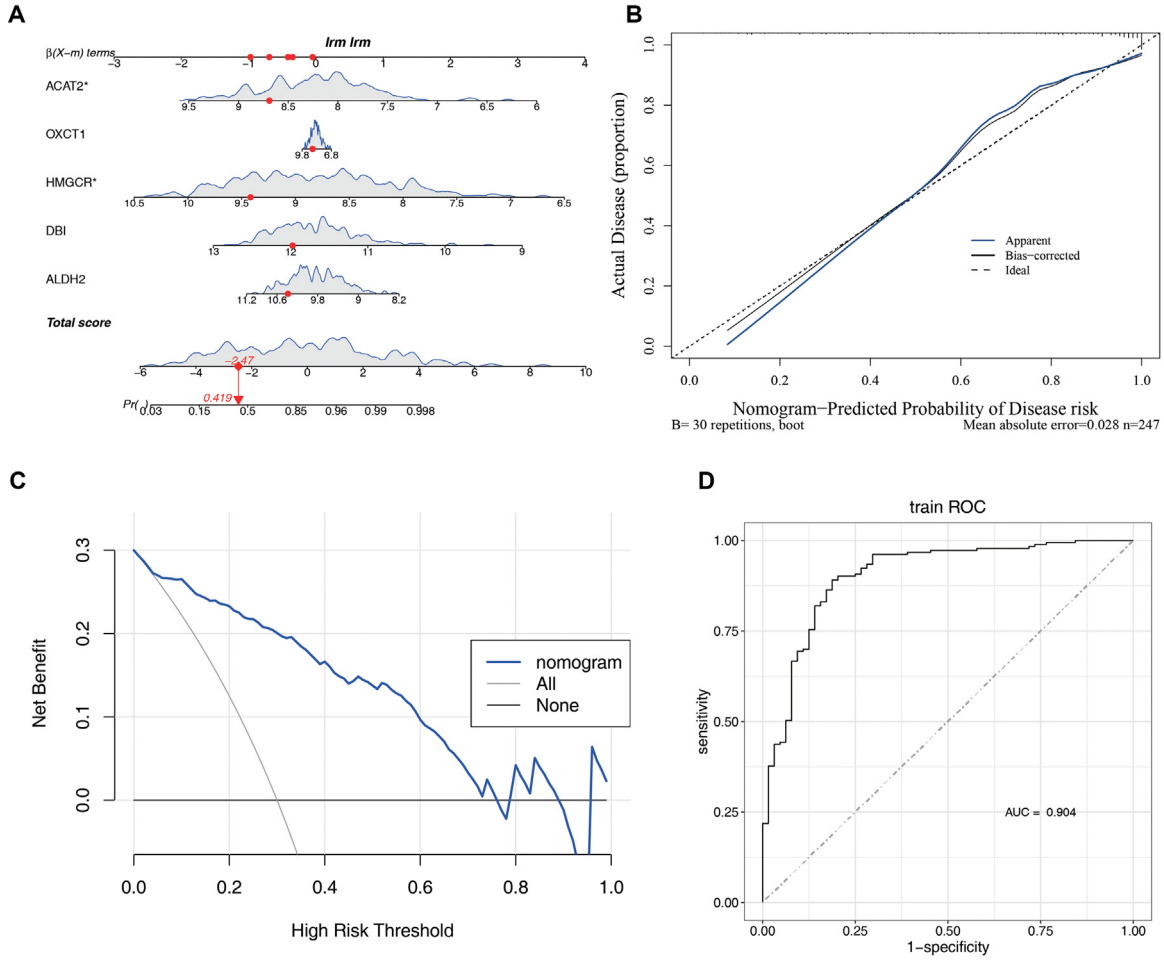

Fig. 5 – Construction and verification of the nomogram model. (A) Nomogram of biomarkers. (B) Calibration curve of nomogram. (C) Decision curve of nomogram. (D) ROC curve of nomogram.

algorithms were intersected to yield eight hub genes (Additional File 1 and Figure 3F).

ALDH2, DBI, HMGCR, OXCT1, and ACAT2 identified as biomarkers

In LASSO regression, a penalty coefficient close to zero helped select features and simplify the model, resulting in six significant genes with lambda.min = 0.016 (Figure 4A). The SVM-RFE algorithm selected features based on their importance, identifying seven significant genes (Figure 4B). Additionally, the Boruta algorithm identified eight significant genes (Figure 4C). Hence, six common genes identified by LASSO, SVM-RFE, and Boruta were selected as key genes: ALDH2, diazepam binding inhibitor (DBI), HMGCR, OXCT1, ACAT2, and VLDLR (Figure 4D). Based on the ROC curves, key genes with AUC > 0.8 (ALDH2, DBI, HMGCR, OXCT1, and ACAT2) in both the training and validation sets were designated as candidate biomarkers (Figure 4E). In both the training and validation cohorts, all five candidate biomarkers were expressed at low levels in the periodontitis group (affected site) and exhibited the same expression trend in both datasets, which led to their adoption as biomarkers (Figure 4F).

Highly predictive of periodontitis using the nomogram model

A nomogram model was developed, indicating that higher total points correlate with an increased likelihood of periodontitis (Figure 5A). Calibration curves with slopes close to 1 reflect a strong agreement between the predicted probabilities of the model and the actual incidence rates (Figure 5B). The net benefit value of the DCA curve was greater than 0, indicating strong predictive performance, while the AUC value of the ROC curve was 0.904, suggesting high predictive accuracy (Figure 5C,D).

Correlation between biomarkers and immune cells infiltration

This study demonstrated immune cell infiltration in both periodontitis and control samples (Figure 6A). There were significant differences between the two sample groups in terms of 15 types of immune cell infiltrations, including memory B cells, naive B cells, resting dendritic cells, M0 macrophages, M1 macrophages, resting mast cells, neutrophils, activated natural killer (NK) cells, resting NK cells, plasma cells, memory-activated CD4 T cells, naive CD4 T cells, CD8 T cells, follicular helper T cells, and gamma delta T cells (Figure 6B). Correlation analysis of biomarkers and

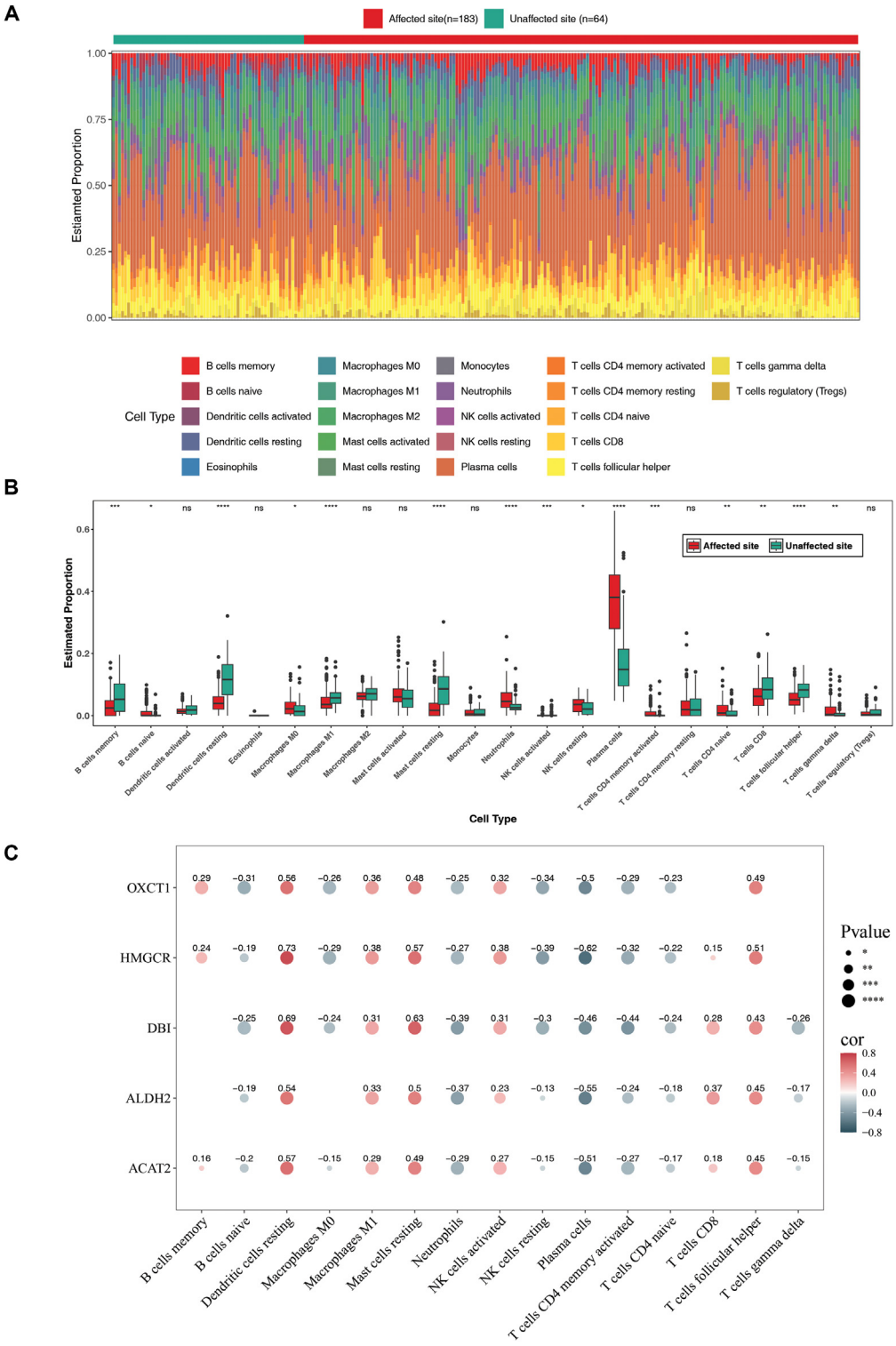

Fig. 6 – Immune infiltration analysis. (A) Heatmap of the composition and abundance of 22 immune cells. The cell abundance of each sample was represented by a column of colour blocks. Different colours represented different cell types, and the height indicated the estimated proportion in the sample. (B) Box-plot of the expression differences of 22 immune cells between PD samples and control samples. Red represented PD samples, and green represented control samples. (C) Heatmap of the correlation matrix between biomarkers and differential immune cells. Blue represented negative correlation, and red represented positive correlation. The deeper the colour, the stronger the correlation; the numbers represented the values of the correlation coefficients, and the size of the dots represented the significance level of the *P* value, from small (not significant) to large (extremely significant).

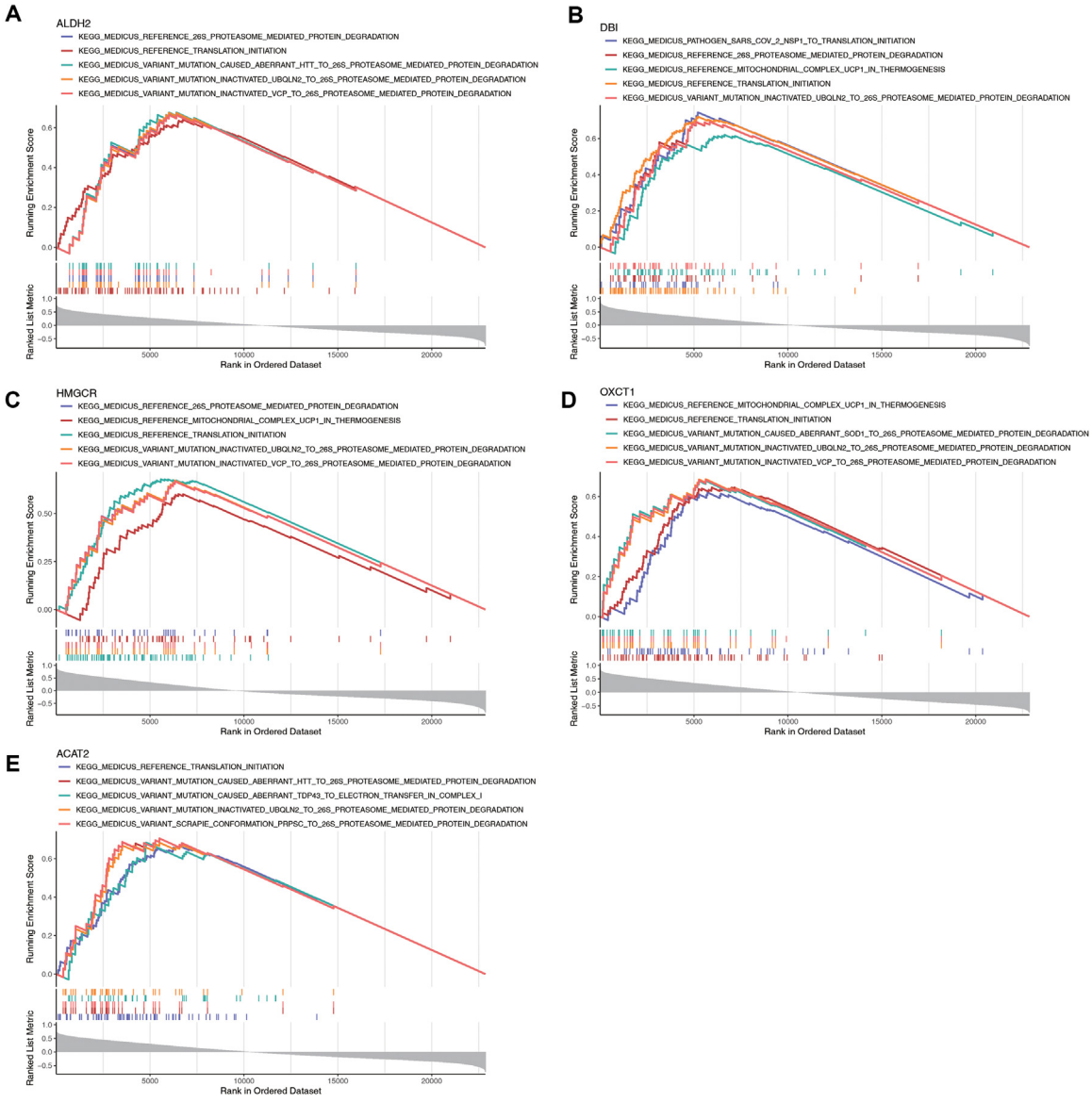

Fig. 7 – Single-gene GSEA analysis chart of biomarkers. (A) ALDH2; (B) DBI; (C) HMGCR; (D) OXCT1; (E) ACAT2.

differential immune cells demonstrated that resting dendritic cells, resting mast cells, and follicular helper T cells were positively correlated with the five biomarkers (Cor > 0.3 and $P < .05$) (Figure 6C).

All five biomarkers worked in 'reference translation initiation' by GSEA

The GSEA results were presented for each biomarker, highlighting the top five enriched pathways ranked by significance (Figure 7A-E). For ALDH2, a total of 157 pathways were enriched, as depicted in Figure 7A. All five biomarkers participated in the 'reference translation initiation' pathway, indicating its significance in the study.

Prediction of biomarker-associated genes, functions, and upstream regulatory molecules

The biomarker-target-pathway network showed how five biomarkers interact with 14 protein-coding genes and nine signalling pathways (Figure 8A). Among the five biomarkers, the pairs with the strongest correlation were HMGCR-OXCT1 and DBI-HMGCR (Figure 8B). The analysis of functional similarity demonstrated that the median values of the biomarkers ranged from 0.25 to 0.50, with distinct median positions for each. This variation indicates differences in the functional similarity of the biomarkers (Figure 8C). Meanwhile, the interquartile range of each biomarker varied greatly, indicating that the distribution of functional similarity was also distinct. Moreover, the gene-

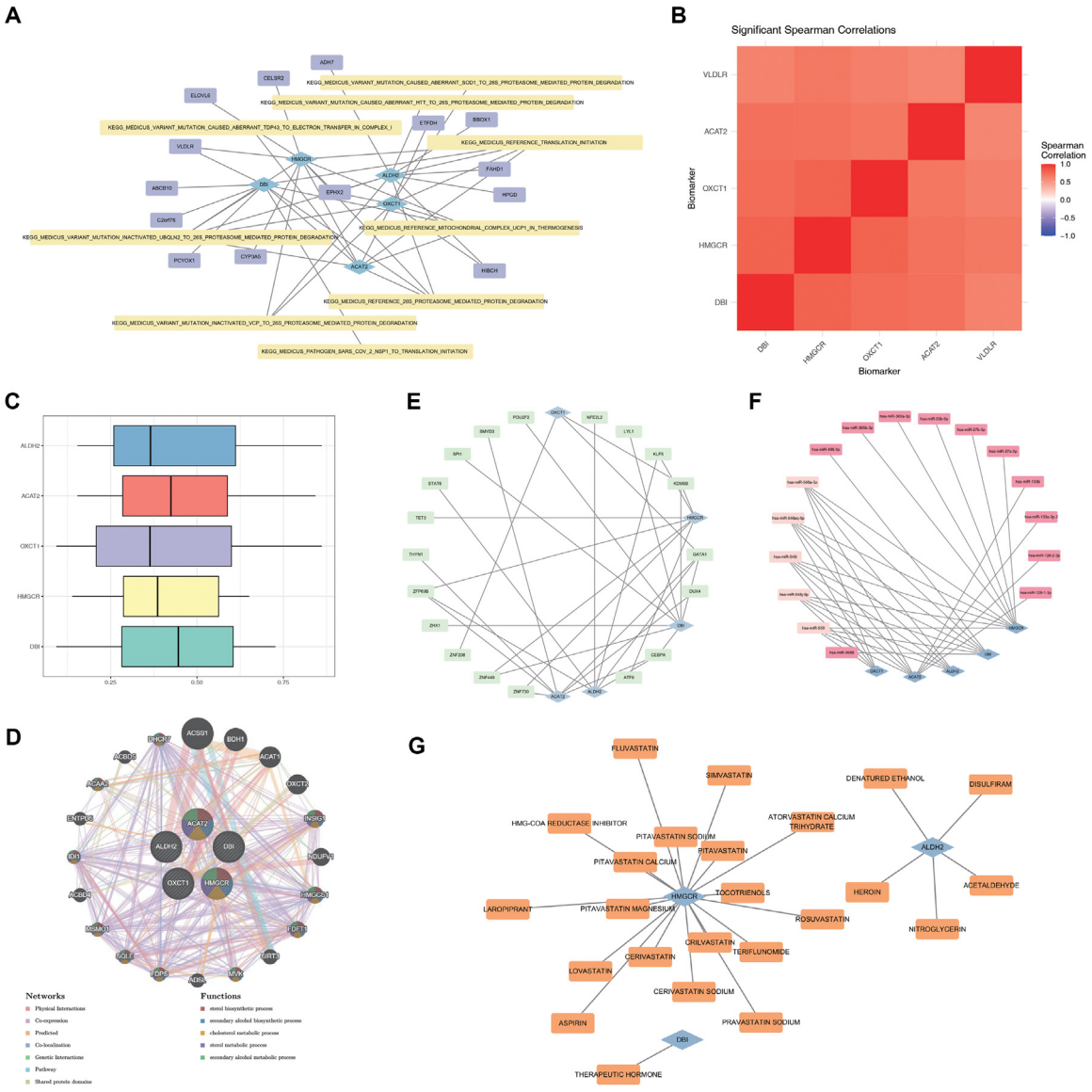

Fig. 8 – Functional-related analysis of biomarkers. (A) Biomarker-target-pathway network. Five blue diamond-shaped nodes each represented a gene, 14 purple rectangular nodes represented a gene encoding a protein, and nine yellow rectangular nodes represented biological pathways, with a total of 46 edges. (B) Correlation between biomarkers. The depth of colour represented the strength of the correlation. Dark red indicated strong positive correlation, light red indicated weak correlation, and blue indicated negative correlation. (C) Box plot of functional similarity analysis of biomarkers. (D) GeneMANIA network of biomarkers. (E) TF-biomarker network graph. Nineteen green rectangular nodes represented transcription factors, and five blue diamond-shaped nodes represented biomarkers, with a total of 31 edges. (F) miRNA-biomarker regulatory network graph. Pink rectangular nodes represented miRNA molecules, 11 dark pink ones were conserved (conserved) miRNAs, and light pink ones were miRNAs coacting on five biomarkers. Five blue diamond-shaped nodes represented biomarkers, with a total of 36 edges. (G) Drug-biomarker relationship network graph. Three blue diamond-shaped nodes represented biomarkers, and 24 orange rectangular nodes represented drugs, with a total of 24 edges.

gene interaction network showcased 20 genes linked to biomarkers involved in BP, including 'sterol biosynthesis' (Figure 8D). Additionally, the TF-biomarker network included 19 TFs predicted by five biomarkers, establishing 31 regulatory relationships (Figure 8E). The miRNA-biomarker network identified 16 miRNAs associated with five biomarkers, including 11 conserved and 5 coacting miRNAs (Figure 8F). Consequently, only three biomarkers (ALDH2, DBI, HMGCR) were relevant to 24 drugs in the drug-biomarker network (Figure 8G).

Biomarkers were lowly expressed in periodontitis group by RT-qPCR

Five biomarkers – ALDH2 ($P = .0017$), DBI ($P = .0395$), HMGCR ($P = .0418$), OXCT1 ($P = .2809$), and ACAT2 ($P = .5054$) – were

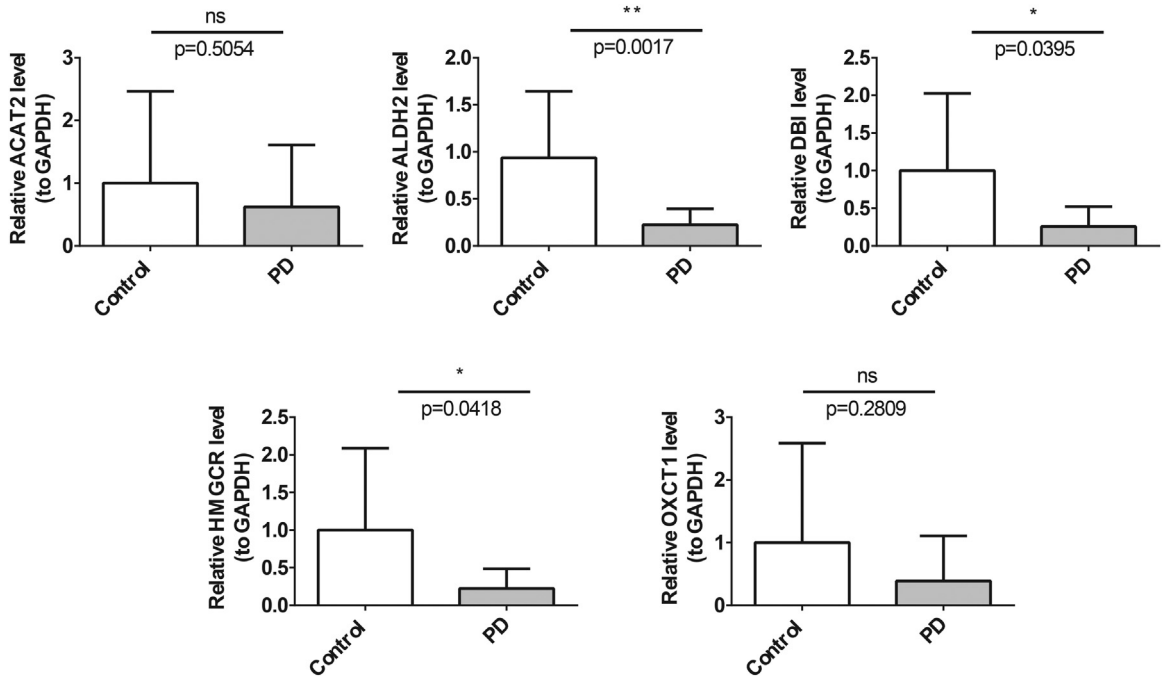

Fig. 9 – Bar graph of RT-qPCR for biomarkers.

expressed at lower levels in the periodontitis group (Figure 9). Specifically, ALDH2, DBI, and HMGCR showed significant differences ($P < .05$) between the periodontitis and control groups.

Discussion

Periodontitis is an oral disease that is difficult to completely cure, characterized by chronic inflammation and tissue destruction in a persistently bacterial environment, which poses significant challenges to treatment. Ferritinophagy is a type of cellular autophagy that regulates intracellular iron metabolism, thereby affecting cell survival and function.[12] Recent studies have found that ferritinophagy plays an important role in the progression of periodontitis.[9] This study, based on periodontitis-related transcriptome data from public databases, utilized bioinformatics analysis to identify biomarkers associated with FRGs in periodontitis. Through screening, five biomarkers were obtained: ALDH2, DBI, HMGCR, OXCT1, and ACAT2.

Aldehyde dehydrogenase 2 family member (ALDH2) is a gene in humans that encodes for mitochondrial aldehyde dehydrogenase.[27] The polymorphism of the ALDH2 gene is associated with various diseases and physiological states, primarily due to its role in degrading harmful aldehyde compounds, thereby reducing oxidative stress and protecting tissues from damage.[28] Meanwhile, ferritinophagy depends on the accumulation of iron and lipid peroxidation, processes that are regulated by oxidative stress. ALDH2 can inhibit ferroptosis by activating nuclear factor erythroid 2-related factor 2 (Nrf2), thereby alleviating inflammatory responses and promoting the osteogenic differentiation of periodontal ligament stem cells in periodontitis.[29] Therefore, this study's findings are consistent with previous research, further emphasizing the importance of ALDH2 as a diagnostic marker for periodontitis.

DBI, also known as Acyl-CoA binding protein, is a multifunctional protein that plays roles in various BP.[30] It has been extensively studied in aspects such as the central nervous system and bioenergy metabolism. First, lipid peroxidation is a key feature of ferritinophagy, as it involves the oxidation of polyunsaturated fatty acids.[31] DBI is involved in the binding and transport of fatty acids, which may affect the supply of fatty acids and thereby indirectly influence the dynamic process of lipid peroxidation even ferritinophagy. Lipid metabolism disorders have a significant impact on inflammatory processes, including periodontitis. On the other hand, the regulation and effects of DBI may be related to the regulation of cellular stress responses, influencing stress response pathways by regulating the utilization and storage of iron, while periodontitis is closely related to oxidative stress.[32] Excessive reactive oxygen species damage cells and produce excessive inflammatory responses in local immunity.[33] If DBI plays a role in antioxidant balance, it can be speculated that it influences the alleviation or acute exacerbation of periodontal disease symptoms.

3-hydroxy-3-methylglaryl-CoA reductase (HMGCR) is the rate-limiting enzyme in the cholesterol synthesis pathway, primarily responsible for the production of cholesterol in the body.[34] Additionally, it plays an important role in the biosynthesis of isoprenoids and lipid metabolism. Disruptions in cholesterol metabolism can affect inflammatory responses.[35] High cholesterol levels are associated with systemic inflammatory responses, which may influence periodontal inflammation through systemic health conditions such as diabetes and hyperlipidemia.[36] Studies have shown that statins can alleviate periodontal inflammation, possibly due to their

anti-inflammatory properties and regulation of cholesterol levels.[37]

3-oxoacid CoA-transferase 1 (OXCT1) plays a critical role in ketone body metabolism, primarily by catalysing the conversion of ketone bodies into acetyl-CoA, which then enters the tricarboxylic acid cycle (TCA cycle) to provide energy.[38] Some studies also suggest that under conditions of oxidative stress and inflammation, cells may increase their utilization of ketone bodies to meet energy demands.[39] This process is particularly important in chronic inflammatory states such as periodontitis, which is accompanied by an increased energy metabolism demand. In such cases, the role of OXCT1 is especially crucial, as it facilitates the key step of converting ketone bodies into energy.[40] Furthermore, ketone bodies are not only intermediates in energy metabolism but have also been found to possess anti-inflammatory properties. For instance, β-hydroxybutyrate, a major ketone body, is believed to inhibit certain inflammatory pathways, reduce oxidative stress, and modulate immune function.[41] These effects may occur indirectly through the action of OXCT1.

Acetyl-CoA cholesterol acyltransferase 2 (ACAT2) is primarily involved in the synthesis of cholesterol esters, playing an important role in lipid metabolism by regulating the balance of free cholesterol and cholesterol esters within cells.[42] Some studies also indicate that ACAT2's regulation of cholesterol esters may affect the cholesterol dynamics in immune cell membranes, thereby influencing immune responses.[43] Cholesterol accumulation can affect the function of immune cells and the intensity of immune responses, potentially acting through the regulation of cell membrane receptors or signalling pathways, thus indirectly impacting the overall response to inflammation.[44,45] Consequently, studying the relationship between ACAT2 and inflammatory markers such as IL-6 and tumour necrosis factor-α can further elucidate its potential role in periodontal diseases. Meanwhile, the study found that these genes were predominantly downregulated in periodontal inflammatory tissues.[46] Such downregulation in periodontitis tissues may further promote the pathological processes of periodontitis through the regulation of energy metabolism, oxidative stress, and other mechanisms.

In this study, by comparing the immune cell infiltration in periodontitis with that in healthy gums, it was revealed that there is a lower level of infiltration of 15 different immune cells in periodontitis patients, including memory B cells, naive B cells, resting dendritic cells and so on. Further analysis of the correlation between biomarkers and differential immune cells showed that resting dendritic cells, resting mast cells, and follicular helper T cells are significantly positively correlated with the five biomarkers, suggesting that the abnormal expression of biomarkers may be related to the dysfunction of immune cell infiltration in periodontitis.

Dendritic cells, as antigen-presenting cells, are responsible for capturing, processing, and presenting antigens to activate T cells. Dendritic cells can mediate inflammation-related bone resorption, which is crucial in the development of periodontitis.[47] Studies have shown that memory B cells participate in immune responses during chronic inflammation of periodontitis by producing specific antibodies, thereby increasing periodontal tissue destruction and accelerating disease progression.[48] Macrophages can be divided into different subtypes based on their activation state. M1 macrophages are associated with proinflammatory responses and play a role in tissue damage and pathogen clearance.[49] Studies have shown that the accumulation of M1 macrophages in periodontitis lesions is associated with tissue destruction and bone resorption, while M2 macrophages are primarily involved in the reparative stage of periodontal inflammation.[50] Mast cells play an important role in immune surveillance and regulating immune responses and may promote inflammatory processes in periodontitis by releasing cytokines and chemokines.[51] Neutrophils are one of the most abundant immune cells in periodontitis, responsible for phagocytosing and clearing pathogens.[52] Studies have shown that persistent neutrophil infiltration can lead to tissue damage and exacerbation of the disease.[53] NK cells combat infections through cytotoxic actions. Through direct interaction with periodontal pathogens, NK cells produce proinflammatory cytokines, which subsequently lead to tissue destruction.[54] In chronic periodontal disease, an increased number of plasma cells may reflect a sustained immune response. Memory-activated and naive CD4 T cells, CD8 T cells, and follicular helper T cells play important roles in regulating immune responses, cellular immunity, and antibody-mediated responses.[55] Dysregulation of CD4 and CD8 T cells may lead to inappropriate inflammatory responses and tissue destruction. Follicular helper T cells assist B cells in producing antibodies and maintaining adaptive immunity.[56] OXCT1 provides energy for activated immune cells, such as T cells and NK cells, by participating in ketone body metabolism.[40] ALDH2 plays a role in the oxidative stress response, regulating the oxidative state of immune cells, thereby affecting the activity of dendritic cells and mast cells, as well as the differentiation and function of follicular helper T cells.[57] DBI is involved in cholesterol metabolism and cell membrane stability, which can influence the antigen-presenting efficiency of dendritic cells and the ability of follicular helper T cells in B cell assistance.[58,59] HMGCR and ACAT2 exert significant effects on T cell activation and proliferation by regulating cholesterol metabolism.[60] In conclusion, these biomarkers may collectively regulate the function and activity of immune cells through pathways involving metabolism, oxidative stress response, and cholesterol homeostasis. Furthermore, their interactions may represent a coordinated response of immune cells in sensing and adapting to their environment. This complex network requires further experimental validation and understanding, ultimately providing better strategies for diagnosing and treating related diseases.

In the occurrence and development of periodontitis, TFs, miRNAs, and related drugs may play roles through various pathways and mechanisms, particularly in connection with the functions of biomarkers and regulatory networks. This study constructed a regulatory network based on five biomarkers, and the results predicted TF KLF5, along with miRNAs such as hsa-miR-495-3p and hsa-miR-27a-3p. KLF5 is a TF belonging to the KLF family, playing essential roles in various BP, including cell proliferation, differentiation, apoptosis, and immune responses. Studies have shown that overexpression of KLF5 can reverse the inhibitory effect of miR-143-3p on osteogenic differentiation, thereby impacting the regeneration and tissue repair of human periodontal ligament cells.[61]

The hsa-miR-495-3p and hsa-miR-27a-3p exert their regulatory functions by binding to the 3′ untranslated region of their mRNA targets. In different cell types and tissues, hsa-miR-495-3p mediates specific biological functions, such as cell proliferation, differentiation, and disease progression, by regulating target gene expression.[62] It also plays a critical role in immune regulation and inflammatory responses. Additionally, some studies have suggested that hsa-miR-495-3p is closely associated with the diagnosis and prognosis of oral squamous cell carcinoma.[63] miR-27a-3p, as a regulatory factor, has been reported to participate in the modulation of inflammatory responses and play a role in regulating osteogenesis-related genes.[64] This is closely linked to the progression of periodontal inflammation and the balance between osteogenesis and bone resorption. It is also believed to be involved in processes such as bone density, bone formation, and periodontal tissue regeneration. Its common targets include genes associated with the Wnt/β-catenin signalling pathway, inflammatory factor pathways, and tumour-related signalling pathways.[65,66] Overall, TFs and miRNAs may exert influence on inflammatory responses and tissue repair processes through gene regulatory networks, playing important roles in the progression of periodontal disease. Investigating the molecular mechanisms and drug-mediated regulatory effects among these can provide new insights and targets for the precision medicine of periodontal disease. Further experimental validation will help to better understand the specific functions and potential therapeutic benefits of these molecules in the disease process of periodontal disease.

The core pathological mechanism of periodontitis is a chronic inflammatory response triggered by bacterial infection, leading to periodontal tissue damage and alveolar bone resorption. Studies have shown that the combined use of omega-3 fatty acids and aspirin can significantly inhibit the expression of inflammatory factors, namely tumour necrosis factor-α and interleukin-1β.[67] These inflammatory factors are key proinflammatory mediators in periodontitis, involved in the activation of immune cells and inflammatory cascades.

In addition, the enzymes COX-2 and iNOS play significant roles in the inflammatory response of periodontitis.[68] COX-2 is associated with the synthesis of prostaglandins, which are critical mediators of bone resorption and tissue destruction in periodontitis.[69] iNOS, on the other hand, aggravates inflammatory responses and oxidative stress by producing excessive nitric oxide (NO).[70] Research has demonstrated that omega-3 fatty acids and aspirin can suppress the protein expression levels of COX-2 and iNOS in RAW264.7 cells.[71]

The RANK/RANKL pathway is the primary regulatory pathway for osteoclast differentiation and activation.[72] Targeting RANK or RANKL can effectively inhibit alveolar bone resorption. Additionally, matrix metalloproteinases (MMPs), such as MMP-9 and MMP-2, play crucial roles in the degradation of periodontal tissues. MMPs are involved in regulating the M1/M2 polarization of macrophages and the Th17/Treg balance of T cells.[73] Therefore, targeting and inhibiting MMPs can reduce the destruction of periodontal tissues. Studies have revealed that the combination of omega-3 fatty acids and aspirin can suppress RANKL-induced MMPs gene expression, thereby mitigating bone resorption and tissue destruction.[71]

The pathological mechanism of periodontitis is complex, involving multiple processes such as inflammatory response, immune regulation, oxidative stress, and abnormal bone metabolism. By inhibiting inflammatory factors, regulating the RANKL/MMP pathway, and exerting antioxidant effects, Omega-3 fatty acids and aspirin work together synergistically, offering a new approach to the treatment of periodontitis.[50] Therefore, future drug development efforts could focus on multitargeted combination therapy strategies.

In this study, we employed various advanced bioinformatics methods and conducted experiments to ultimately identify five diagnostic biomarkers for periodontitis. Furthermore, this discovery may have potential significance in the diagnosis and further research of periodontitis. Nonetheless, this study also has several limitations to be addressed in future research. First, the sample size in this study is relatively small, and it may influence the generalization and representativeness of the results. The data from the GEO database is limited, which might enhance individual differences and bring potential biases to the findings. Consequently, future research should concentrate on enlarging the sample size, especially by including individuals of various age groups, genders, and disease subtypes, to enhance the wide applicability of the results. Second, this study primarily focused on analyzing gene expression levels, while insufficiently exploring protein levels and their functions. As proteins directly perform the biological functions of genes, future studies can integrate multiomic analyses for more comprehensive investigation of the roles of key genes in the pathogenesis and progression of the disease. Furthermore, although this study examined the variations in immune cell infiltration, the particular functions of diverse immune cell subgroups and their connections with diagnostic biomarkers have not been fully explored. Future research should further concentrate on the mechanisms through which immune cells contribute to periodontitis, especially the interactions among different immune cell subpopulations and biomarkers, in order to disclose more elaborate immune regulatory networks. The conclusions of this study support the potential of ferritin clearance to alleviate oxidative stress and protect cells. However, note that these conclusions were obtained under specific experimental conditions. Future research can further investigate the dual effects of ferritinophagy and degradation through modulating intracellular iron levels and oxidative stress environments. This will help provide more detailed insights into their mechanisms of action under different conditions.

To overcome these limitations, future studies can be enhanced in several ways. First, the sample population scope can be expanded. This can be achieved by using more extensive datasets and conducting multicentre cohort studies to observe disease characteristic differences among various populations. Second, new technological methods, like single-cell RNA sequencing and spatial transcriptomics, can be used to determine more detailed gene interaction networks and investigate the spatial and temporal dynamic connections of genes in diseases. Lastly, in the case of chronic diseases like periodontitis, long-term longitudinal studies should be planned to observe the dynamic alterations in gene expression and their connection with disease progression.

Conclusion

In conclusion, ALDH2, DBI, HMGCR, OXCT1, and ACAT2 have been identified as diagnostic biomarkers for periodontitis, with these five biomarkers being closely associated with the occurrence and progression of the disease. Meanwhile, there is an imbalance in immune cell infiltration in periodontitis. Our study provides new insights into the potential mechanisms of periodontitis and the development of therapeutic targets.

Data availability

The datasets analysed during the current study are available in the [Gene Expression Omnibus (GEO)] repository, [https://www.ncbi.nlm.nih.gov/geo/]; [GeneCards] [https://www.genecards.org/]; [GeneMANIA] repository, [http://genemania.org/]; [ChEA3] repository, [https://maayanlab.cloud/chea3/]; [GmiRanda] repository, [http://www.microrna.org]; [Drug Gene Interaction (DGIdb)] repository, [http://www.dgidb.org]; and [TargetScan] repository, [https://www.targetscan.org/vert_80/].

Conflict of interest

The authors declare no competing interests with respect to the research, authorship, and/or publication of this article.

Funding

All phases of this study were supported by the Scientific Research Innovation Project – Hubei Province Key Laboratory of Oral and Maxillofacial Development and Regeneration (grant number: 2022kqhm008); Intramural Research Fund of the First Affiliated Hospital of Xinjiang Medical University (grant number: 2024YFY-QKQN-26).

Ethics statement and consent to participate

The present study was approved by the Ethics Committee of the First Affiliated Hospital of Xinjiang Medical University (approval no. IACUC-JT-20231121-12). Procedures operated in this research were completed in keeping with the standards set out in the Announcement of Helsinki and laboratory guidelines of research in China. Written informed consent to participate in this study was provided by the participants or legal guardian/next of kin and the study design adhered to the ethical principles outlined in the Declaration of Helsinki.

Clinical relevance

In the coming decades, indeed, the burden of periodontitis is anticipated to persist as a concern. If a study identifies a new marker for periodontal disease progression, it could lead to better diagnosis. It could also contribute to more efficient treatment and preventive strategies, ultimately enhancing patients' periodontal health.

Author contributions

Conceptualization: Chen-Xi Li. Writing – original draft: Yi-Ming Li, Chen-Xi Li. Writing – revision, review & editing: Chen-Xi Li. Data curation: Yi-Ming Li, Chen-Xi Li. Formal analysis: Yi-Ming Li, Chen-Xi Li. Funding acquisition: Chen-Xi Li, Reyila Jureti. Investigation: Yi-Ming Li, Chen-Xi Li, Reyila Jureti, Gulinuer Awuti. Methodology: Chen-Xi Li. Supervision: Chen-Xi Li, Gulinuer Awuti. Validation: Yi-Ming Li, Reyila Jureti, Gulinuer Awuti. Project administration: Chen-Xi Li. All authors read and approved the final manuscript. All authors contributed to the article and approved the submitted version.

Acknowledgements

Authors appreciate all financial support that granted and are also grateful to the research volunteer and collaborators. Many thanks for Sonnig Biomedical Studio, Urumqi, China as that team was so kind to perform bioinformatics analyses.

Supplementary materials

Supplementary material associated with this article can be found in the online version at doi:10.1016/j.identj.2025.03.011.

REFERENCES

1. Genco RJ, Sanz M. Clinical and public health implications of periodontal and systemic diseases: an overview. Periodontol 2000 2020;83(1):7–13. doi: 10.1111/prd.12344.
2. Villoria GEM, Fischer RG, Tinoco EMB, et al. Periodontal disease: a systemic condition. Periodontol 2000 2024;96(1):7–19. doi: 10.1111/prd.12616.
3. Kim TH, Heo SY, Chandika P, et al. A literature review of bioactive substances for the treatment of periodontitis: in vitro, in vivo and clinical studies. Heliyon 2024;10(2):e24216. doi: 10.1016/j.heliyon.2024.e24216.
4. Santos MS, Silva JC, Carvalho MS. Hierarchical biomaterial scaffolds for periodontal tissue engineering: recent progress and current challenges. Int J Mol Sci 2024;25(16):8562. doi: 10.3390/ijms25168562.
5. Ashfaq R, Kovács A, Berkó S, et al. Developments in alloplastic bone grafts and barrier membrane biomaterials for periodontal guided tissue and bone regeneration therapy. Int J Mol Sci 2024;25(14):7746. doi: 10.3390/ijms25147746.
6. Xu XY, Li X, Wang J, et al. Concise review: periodontal tissue regeneration using stem cells: strategies and translational considerations. Stem Cells Transl Med 2019;8(4):392–403. doi: 10.1002/sctm.18-0181.
7. Liu Y, Guo L, Li X, et al. Challenges and tissue engineering strategies of periodontal-guided tissue regeneration. Tissue Eng Part C Methods 2022;28(8):405–19. doi: 10.1089/ten.TEC.2022.0106.
8. Li JY, Feng YH, Li YX, et al. Ferritinophagy: a novel insight into the double-edged sword in ferritinophagy-ferroptosis axis and human diseases. Cell Prolif 2024;57(7):e13621. doi: 10.1111/cpr.13621.
9. Guo W, Zhao Y, Li H, et al. NCOA4-mediated ferritinophagy promoted inflammatory responses in periodontitis. J Periodontal Res 2021;56(3):523–34. doi: 10.1111/jre.12852.

10. Zhao Y, Li J, Guo W, et al. Periodontitis-level butyrate-induced ferroptosis in periodontal ligament fibroblasts by activation of ferritinophagy. Cell Death Discov 2020;6(1):119. doi: 10.1038/s41420-020-00356-1.
11. Kawabata H, Miyazawa N, Matsuda Y, et al. Measurement of serum hepcidin-25 by latex agglutination in healthy volunteers and patients with hematologic disorders. Int J Hematol 2024;119(4):392–8. doi: 10.1007/s12185-024-03720-4.
12. Tang M, Chen Z, Wu D, et al. Ferritinophagy/ferroptosis: iron-related newcomers in human diseases. J Cell Physiol 2018;233 (12):9179–90. doi: 10.1002/jcp.26954.
13. Ritchie ME, Phipson B, Wu D, et al. limma powers differential expression analyses for RNA-sequencing and microarray studies. Nucleic Acids Res 2015;43(7):e47. doi: 10.1093/nar/gkv007.
14. Hänzelmann S, Castelo R, Guinney J. GSVA: gene set variation analysis for microarray and RNA-seq data. BMC Bioinform 2013;14:7. doi: 10.1186/1471-2105-14-7.
15. Langfelder P, Horvath S. WGCNA: an R package for weighted correlation network analysis. BMC Bioinform 2008;9:559. doi: 10.1186/1471-2105-9-559.
16. Wu T, Hu E, Xu S, et al. clusterProfiler 4.0: a universal enrichment tool for interpreting omics data. Innovation (Camb) 2021;2(3):100141. doi: 10.1016/j.xinn.2021.100141.
17. Friedman J, Hastie T, Tibshirani R. Regularization paths for generalized linear models via coordinate descent. J Stat Softw 2010;33(1):1–22.
18. Scrucca L, Raftery AE. clustvarsel: a package implementing variable selection for gaussian model-based clustering in R. J Stat Softw 2018;84:1. doi: 10.18637/jss.v084.i01.
19. Robin X, Turck N, Hainard A, et al. pROC: an open-source package for R and S+ to analyze and compare ROC curves. BMC Bioinform 2011;12:77. doi: 10.1186/1471-2105-12-77.
20. Vickers AJ, Elkin EB. Decision curve analysis: a novel method for evaluating prediction models. Med Decis Making 2006;26 (6):565–74. doi: 10.1177/0272989X06295361.
21. Chen B, Khodadoust MS, Liu CL, et al. Profiling tumor infiltrating immune cells with CIBERSORT. Methods Mol Biol 2018;1711:243–59. doi: 10.1007/978-1-4939-7493-1_12.
22. Grieder S, Steiner MD. Algorithmic jingle jungle: a comparison of implementations of principal axis factoring and promax rotation in R and SPSS. Behav Res Methods 2022;54(1):54–74. doi: 10.3758/s13428-021-01581-x.
23. Lee CY, Bu LX, DeBenedetti A, et al. Transcriptional and translational dual-regulated oncolytic herpes simplex virus type 1 for targeting prostate tumors. Mol Ther 2010;18(5):929–35. doi: 10.1038/mt.2010.26.
24. Bachtiar BM, Haerani N, Soeroso Y, et al. The presence of ACE2 and regulatory miRNAs (miR-200c-3p and miR-421-5p) in the saliva of periodontitis patients post-COVID-19 vaccination. Front Dent Med 2024;5:1438139. doi: 10.3389/fdmed.2024.1438139.
25. Jiang H, Xi Y, Jiang Q, et al. LRP5 down-regulation exacerbates inflammation and alveolar bone loss in periodontitis by inhibiting PI3K/c-FOS signalling. J Clin Periodontol 2025;52(4):637–50. doi: 10.1111/jcpe.14112.
26. Raza M, Abud DG, Wang J, et al. Ease and practicability of the 2017 classification of periodontal diseases and conditions: a study of dental electronic health records. BMC Oral Health 2024;24(1):621. doi: 10.1186/s12903-024-04385-5.
27. Chen J, Hu C, Lu X, et al. ALDH2 alleviates inflammation and facilitates osteogenic differentiation of periodontal ligament stem cells in periodontitis by blocking ferroptosis via activating Nrf2. Funct Integr Genomics 2024;24(5):184. doi: 10.1007/s10142-024-01465-1.
28. Patil RT, Dhadse PV, Salian SS, et al. Role of oxidative stress in periodontal diseases. Cureus 2024;16(5):e60779. doi: 10.7759/cureus.60779.
29. Lu H, Zheng Y, Wang D. ATF3 affects osteogenic differentiation in inflammatory hPDLSCs by mediating ferroptosis via regulating the Nrf2/HO-1 signaling pathway. Tissue Cell 2024;89:102447. doi: 10.1016/j.tice.2024.102447.
30. Motiño O, Lambertucci F, Anagnostopoulos G, et al. ACBP/DBI protein neutralization confers autophagy-dependent organ protection through inhibition of cell loss, inflammation, and fibrosis. Proc Natl Acad Sci USA 2022;119(41):e2207344119. doi: 10.1073/pnas.2207344119.
31. Rochette L, Dogon G, Rigal E, et al. Lipid peroxidation and iron metabolism: two corner stones in the homeostasis control of ferroptosis. Int J Mol Sci 2022;24(1):449. doi: 10.3390/ijms24010449.
32. Kocaman G, Altinoz E, Erdemli ME, et al. Crocin attenuates oxidative and inflammatory stress-related periodontitis in cardiac tissues in rats. Adv Clin Exp Med 2021;30(5):517–24. doi: 10.17219/acem/133753.
33. Yamaguchi T, Yamamoto Y, Egashira K, et al. Oxidative stress inhibits endotoxin tolerance and may affect periodontitis. J Dent Res 2023;102(3):331–9. doi: 10.1177/00220345221138523.
34. Iacono G, Abay A, Murillo JSG, et al. Differentiating erythroblasts adapt to mechanical stimulation by upregulation of cholesterol biosynthesis via S1P/SREBP-induced HMGCR expression. Sci Rep 2024;14(1):30157. doi: 10.1038/s41598-024-81746-8.
35. Leng E, Xiao Y, Mo Z, et al. Synergistic effect of phytochemicals on cholesterol metabolism and lipid accumulation in HepG2 cells. BMC Complement Altern Med 2018;18(1):122. doi: 10.1186/s12906-018-2189-6.
36. Govaere O, Petersen SK, Martinez-Lopez N, et al. Macrophage scavenger receptor 1 mediates lipid-induced inflammation in non-alcoholic fatty liver disease. J Hepatol 2022;76(5):1001–12. doi: 10.1016/j.jhep.2021.12.012.
37. Hu N, Chen C, Wang J, et al. Atorvastatin ester regulates lipid metabolism in hyperlipidemia rats via the PPAR-signaling pathway and HMGCR expression in the liver. Int J Mol Sci 2021;22(20):11107. doi: 10.3390/ijms222011107.
38. Zhu CX, Yan K, Chen L, et al. Targeting OXCT1-mediated ketone metabolism reprograms macrophages to promote antitumor immunity via CD8+ T cells in hepatocellular carcinoma. J Hepatol 2024;81(4):690–703. doi: 10.1016/j.jhep.2024.05.007.
39. Fukao T, Mitchell G, Sass JO, et al. Ketone body metabolism and its defects. J Inherit Metab Dis 2014;37(4):541–51. doi: 10.1007/s10545-014-9704-9.
40. Dong YN, Mesaros C, Xu P, et al. Frataxin controls ketone body metabolism through regulation of OXCT1. PNAS Nexus 2022;1 (3):pgac142. doi: 10.1093/pnasnexus/pgac142.
41. Vargas-López M, Quiroz-Vicente CA, Pérez-Hernández N, et al. The ketone body β-hydroxybutyrate as a fuel source of chondrosarcoma cells. Heliyon 2024;10(9):e30212. doi: 10.1016/j.heliyon.2024.e30212.
42. Parini P, Jiang ZY, Einarsson C, et al. ACAT2 and human hepatic cholesterol metabolism: identification of important gender-related differences in normolipidemic, non-obese Chinese patients. Atherosclerosis 2009;207(1):266–71. doi: 10.1016/j.atherosclerosis.2009.04.010.
43. Ma Z, Huang Z, Zhang C, et al. Hepatic Acat2 overexpression promotes systemic cholesterol metabolism and adipose lipid metabolism in mice. Diabetologia 2023;66(2):390–405. doi: 10.1007/s00125-022-05829-9.
44. Zimmer S, Grebe A, Bakke SS, et al. Cyclodextrin promotes atherosclerosis regression via macrophage reprogramming. Sci Transl Med 2016;8(333):333ra50. doi: 10.1126/scitranslmed.aad6100.
45. Singh V, Kaur R, et al. ICAM-1 and VCAM-1: Gatekeepers in various inflammatory and cardiovascular disorders. Clin Chim Acta 2023;548:117487. doi: 10.1016/j.cca.2023.117487.

46. Pashaei M, Farhadi E, Kavosi H, et al. Talabostat, fibroblast activation protein inhibitor, attenuates inflammation and fibrosis in systemic sclerosis. Inflammopharmacology 2024;32 (5):3181–93. doi: 10.1007/s10787-024-01536-6.
47. Wu L, Luo Z, Chen Y, et al. Butyrate inhibits dendritic cell activation and alleviates periodontitis. J Dent Res 2023;102 (12):1326–36. doi: 10.1177/00220345231187824.
48. Han YK, Jin Y, Miao YB, et al. Improved RANKL production by memory B cells: a way for B cells promote alveolar bone destruction during periodontitis. Int Immunopharmacol 2018;64:232–7. doi: 10.1016/j.intimp.2018.08.033.
49. Luo W, Du C, Huang H, et al. The role of macrophage death in periodontitis: a review. Inflammation 2024;47(6):1889–901. doi: 10.1007/s10753-024-02015-4.
50. Lin B, Fan Y, Yang X, et al. MMP-12 and periodontitis: unraveling the molecular pathways of periodontal tissue destruction. J Inflamm Res 2024;17:7793–806. doi: 10.2147/JIR.S480466.
51. Trimarchi M, Lauritano D, Ronconi G, et al. Mast cell cytokines in acute and chronic gingival tissue inflammation: role of IL-33 and IL-37. Int J Mol Sci 2022;23(21):13242. doi: 10.3390/ijms232113242.
52. Jing L, Kim S, Sun L, et al. IL-37- and IL-35/IL-37-producing plasma cells in chronic periodontitis. J Dent Res 2019;98 (7):813–21. doi: 10.1177/0022034519847443.
53. Das S, Singh S, Kumar A. Bacterial burden declines but neutrophil infiltration and ocular tissue damage persist in experimental staphylococcus epidermidis endophthalmitis. Front Cell Infect Microbiol 2021;11:780648. doi: 10.3389/fcimb.2021.780648.
54. Wilensky A, Chaushu S, Shapira L. The role of natural killer cells in periodontitis. Periodontol 2000 2015;69(1):128–41. doi: 10.1111/prd.12092.
55. Li W, Zhang Z, Wang ZM. Differential immune cell infiltrations between healthy periodontal and chronic periodontitis tissues. BMC Oral Health 2020;20(1):293. doi: 10.1186/s12903-020-01287-0.
56. Wei H, Xie A, Li J, et al. PD-1+ CD4 T cell immune response is mediated by HIF-1α/NFATc1 pathway after *P. yoelii* infection. Front Immunol 2022;13:942862. doi: 10.3389/fimmu.2022.942862.
57. Yao S, Yin X, Chen T, et al. ALDH2 is a prognostic biomarker and related with immune infiltrates in HCC. Am J Cancer Res 2021;11(11):5319–37 2156-6976/ajcr0139655.
58. Sica V, Martins I, Pietrocola F, et al. Quantification of intracellular ACBP/DBI levels. Methods Cell Biol 2021;165:111–22. doi: 10.1016/bs.mcb.2020.12.004.
59. Demoersman J, Pers JO. Update on B cell response in periodontitis. Adv Exp Med Biol 2022;1373:175–93. doi: 10.1007/978-3-030-96881-6_9.
60. Ibrahim A, Shafie NH, Mohd Esa N, et al. Mikania micrantha extract inhibits HMG-CoA reductase and ACAT2 and ameliorates hypercholesterolemia and lipid peroxidation in high cholesterol-fed rats. Nutrients 2020;12(10):3077. doi: 10.3390/nu12103077.
61. Wangzhou K, Lai Z, Lu Z, et al. MiR-143-3p inhibits osteogenic differentiation of human periodontal ligament cells by targeting KLF5 and inactivating the Wnt/β-catenin pathway. Front Physiol 2021;11:606967. doi: 10.3389/fphys.2020.606967.
62. Li D, Knox B, Chen S, et al. MicroRNAs hsa-miR-495-3p and hsa-miR-486-5p suppress basal and rifampicin-induced expression of human sulfotransferase 2A1 (SULT2A1) by facilitating mRNA degradation. Biochem Pharmacol 2019;169: 113617. doi: 10.1016/j.bcp.2019.08.019.
63. Chen X, Lei H, Cheng Y, et al. CXCL8, MMP12, and MMP13 are common biomarkers of periodontitis and oral squamous cell carcinoma. Oral Dis 2024;30(2):390–407. doi: 10.1111/odi.14419.
64. Karri RL, Amrutha R, Shrinivas, et al., et al. Analyzing pooled microarray gene expression data to uncover common pathways in periodontitis and oral squamous cell carcinoma from the gene expression omnibus. J Pharm Bioallied Sci 2024;16 (Suppl 2):S1515–21. doi: 10.4103/jpbs.jpbs_1180_23.
65. Güney Z, Kurgan Ş, Önder C, et al. Wnt signaling in periodontitis. Clin Oral Investig 2023;27(11):6801–12. doi: 10.1007/s00784-023-05294-7.
66. Duan P, Bonewald LF. The role of the wnt/β-catenin signaling pathway in formation and maintenance of bone and teeth. Int J Biochem Cell Biol 2016;77(Pt A):23–9. doi: 10.1016/j.biocel.2016.05.015.
67. El-Sharkawy H, Aboelsaad N, Eliwa M, et al. Adjunctive treatment of chronic periodontitis with daily dietary supplementation with omega-3 fatty acids and low-dose aspirin. J Periodontol 2010;81(11):1635–43. doi: 10.1902/jop.2010.090628.
68. Costantini E, Sinjari B, Falasca K, et al. Assessment of the vanillin anti-inflammatory and regenerative potentials in inflamed primary human gingival fibroblast. Mediators Inflamm 2021;2021:5562340. doi: 10.1155/2021/5562340.
69. Butucel E, Balta I, Bundurus IA, et al. Natural antimicrobials promote the anti-oxidative inhibition of COX-2 mediated inflammatory response in primary oral cells infected with *Staphylococcus aureus*, *Streptococcus pyogenes* and *Enterococcus faecalis*. Antioxidants (Basel) 2023;12(5):1017. doi: 10.3390/antiox12051017.
70. Pan X, Shao Y, Wang F, et al. Protective effect of apigenin magnesium complex on H2O2-induced oxidative stress and inflammatory responses in rat hepatic stellate cells. Pharm Biol 2020;58(1):553–60. doi: 10.1080/13880209.2020.1772840.
71. Yang M, Li L, Soh Y, et al. Effects of omega-3 fatty acids and aspirin on *Porphyromonas gingivalis*-induced periodontitis in rats. J Periodontol 2019;90(11):1307–19. doi: 10.1002/JPER.19-0063.
72. Liang J, Liu L, Feng H, et al. Therapeutics of osteoarthritis and pharmacological mechanisms: a focus on RANK/RANKL signaling. Biomed Pharmacother 2023;167:115646. doi: 10.1016/j.biopha.2023.115646.
73. Neprelyuk OA, Zhad'ko SI, Romanenko IG, et al. Adjunctive use of omega-3 fatty acids in combination with low-dose aspirin in periodontitis: systematic review and meta-analysis. J Periodontal Res 2023;58(6):1128–38. doi: 10.1111/jre.13191.